

The Lattice Free Energy of QCD with Clover Fermions, up to Three-Loops

A. Athenodorou^a, H. Panagopoulos^b and A. Tsapalis^c

^a*Rudolf Peierls Centre for Theoretical Physics, University of Oxford,
1 Keble Road, Oxford, OX1 3NP, U.K.*

^b*Department of Physics, University of Cyprus,
P.O. Box 20537, Nicosia CY-1678, Cyprus*

^c*Institute of Accelerating Systems and Applications,
University of Athens, Greece*

email: a.Athenodorou1@physics.ox.ac.uk, haris@ucy.ac.cy, a.tsapalis@iasa.gr
(February 5, 2008)

Abstract

We calculate the perturbative value of the free energy in Lattice QCD, up to three loops. Our calculation is performed using Wilson gluons and the Sheikholeslami - Wolhert (clover) improved action for fermions.

The free energy is directly related to the average plaquette. To carry out the calculation, we compute all relevant Feynman diagrams up to 3 loops, using a set of automated procedures in Mathematica; numerical evaluation of the resulting loop integrals is performed on finite lattice, with subsequent extrapolation to infinite size.

The results are presented as a function of the fermion mass m , for any $SU(N_c)$ gauge group, and for an arbitrary number of fermion flavors. In order to enable independent comparisons, we also provide the results on a *per diagram* basis, for a specific mass value.

Keywords: Lattice perturbation theory, Free energy, Average plaquette, Clover action,

PACS numbers: 11.15.Ha, 12.38.Gc, 12.38.Bx

I. FORMULATION OF THE PROBLEM

In this work we calculate the free energy of QCD on the lattice, up to three loops in perturbation theory. We employ Wilson gluons and the $\mathcal{O}(a)$ improved Sheikholeslami-Wohlert (clover) [1] action for fermions. The purpose of this action is to reduce finite lattice spacing effects, leading to a faster approach to the continuum. Dynamical simulations employing the clover action are currently in progress by the CP-PACS/JLQCD [2] and UKQCD/CLS [3] collaborations and therefore perturbative studies of properties of the QCD action with clover quarks are worthy of being undertaken. The free energy, in the simpler case of Wilson fermions, was studied in [4].

The free energy in QCD on the lattice can be related to the average plaquette. The results find several applications, for example: a) In improved scaling schemes, using an appropriately defined effective coupling which depends on the average plaquette (see, e. g., [5,6]), b) In long standing efforts, starting with [7], to determine the value of the gluon condensate, c) In studies of the interquark potential [8], and d) As a test of perturbation theory, at its limits of applicability.

Indeed, regarding point (d) above, the plaquette expectation value is a prototype for additive renormalization of a composite, dimensionful operator. The vacuum diagrams contributing to such a calculation are power divergent in the lattice spacing and may well dominate over any nonperturbative signal in a numerical simulation.

Starting from the Wilson formulation of QCD on the lattice, with the addition of the clover (SW) fermion term, the action reads in standard notation:

$$\begin{aligned}
S_L &\equiv S_G + S_F, \\
S_G &= \frac{1}{g^2} \sum_{x, \mu, \nu} \text{Tr} [1 - U_{\mu, \nu}(x)], \\
S_F &= \sum_f \sum_x (4r + m_B) \bar{\psi}_f(x) \psi_f(x) \\
&\quad - \frac{1}{2} \sum_f \sum_{x, \mu} [\bar{\psi}_f(x) (r - \gamma_\mu) U_\mu(x) \psi_f(x + \hat{\mu}) + \bar{\psi}_f(x + \hat{\mu}) (r + \gamma_\mu) U_\mu(x)^\dagger \psi_f(x)] \\
&\quad + \frac{i}{4} c_{\text{SW}} \sum_f \sum_{x, \mu, \nu} \bar{\psi}_f(x) \sigma_{\mu\nu} \hat{F}_{\mu\nu}(x) \psi_f(x)
\end{aligned} \tag{1}$$

$$\text{where :} \quad \hat{F}_{\mu\nu} \equiv \frac{1}{8} (Q_{\mu\nu} - Q_{\nu\mu}), \quad Q_{\mu\nu} = U_{\mu, \nu} + U_{\nu, -\mu} + U_{-\mu, -\nu} + U_{-\nu, \mu} \tag{2}$$

Here $U_{\mu, \nu}(x)$ is the usual product of $SU(N_c)$ link variables $U_\mu(x)$ along the perimeter of a plaquette in the μ - ν directions, originating at x ; g denotes the bare coupling constant; r is the Wilson parameter, which will be assigned its standard value $r = 1$; f is a flavor index; $\sigma_{\mu\nu} = (i/2)[\gamma_\mu, \gamma_\nu]$. Powers of the lattice spacing a have been omitted and may be directly reinserted by dimensional counting.

The clover coefficient c_{SW} is a free parameter for the purposes of the present calculation and our results will be presented as a polynomial in c_{SW} , with coefficients which we compute. Preferred values for c_{SW} have been suggested by both perturbative (1-loop) [1] and non-perturbative [9] studies.

We use the standard covariant gauge-fixing term [10]; in terms of the vector field $Q_\mu(x)$ [$U_\mu(x) = \exp(i g Q_\mu(x))$], it reads:

$$S_{\text{gf}} = \lambda_0 \sum_{\mu, \nu} \sum_x \text{Tr} \Delta_\mu^- Q_\mu(x) \Delta_\nu^- Q_\nu(x), \quad \Delta_\mu^- Q_\nu(x) \equiv Q_\nu(x - \hat{\mu}) - Q_\nu(x) \quad (3)$$

Having to compute a gauge invariant quantity, we chose to work in the Feynman gauge, $\lambda_0 = 1$. Covariant gauge fixing produces the following action for the ghost fields ω and $\bar{\omega}$

$$S_{\text{gh}} = 2 \sum_{x, \mu} \text{Tr} \left\{ \left(\Delta_\mu^+ \omega(x) \right)^\dagger \left(\Delta_\mu^+ \omega(x) + i g_0 [Q_\mu(x), \omega(x)] + \frac{i g_0}{2} [Q_\mu(x), \Delta_\mu^+ \omega(x)] \right. \right. \\ \left. \left. - \frac{g_0^2}{12} [Q_\mu(x), [Q_\mu(x), \Delta_\mu^+ \omega(x)]] \right. \right. \\ \left. \left. - \frac{g_0^4}{720} [Q_\mu(x), [Q_\mu(x), [Q_\mu(x), [Q_\mu(x), \Delta_\mu^+ \omega(x)]]]] \right] + \dots \right\}, \\ \Delta_\mu^+ \omega(x) \equiv \omega(x + \hat{\mu}) - \omega(x) \quad (4)$$

Finally the change of integration variables from links to vector fields yields a jacobian that can be rewritten as the usual measure term S_m in the action:

$$S_m = \sum_{x, \mu} \left\{ \frac{N_c g_0^2}{12} \text{Tr} \{ (Q_\mu(x))^2 \} + \frac{N_c g_0^4}{1440} \text{Tr} \{ (Q_\mu(x))^4 \} + \frac{g_0^4}{480} \left(\text{Tr} \{ (Q_\mu(x))^2 \} \right)^2 + \dots \right\} \quad (5)$$

In S_{gh} and S_m we have written out only terms relevant to our computation. The full action is:

$$S = S_L + S_{\text{gf}} + S_{\text{gh}} + S_m \quad (6)$$

The average value of the action density, S/V , is directly related to the average plaquette. For the gluon part we have:

$$\langle S_G/V \rangle = 6 \beta E_G, \quad E_G \equiv 1 - \frac{1}{N_c} \text{Tr} \langle U_{\mu, \nu}(x) \rangle, \quad \beta = 2 N_c / g^2 \quad (7)$$

As for $\langle S_F/V \rangle$, it is trivial in any action which is bilinear in the fermion fields, and leads to:

$$\langle S_F/V \rangle = -4 N_c N_f \quad (8)$$

(N_f : number of fermion flavors).

We will calculate E_G in perturbation theory:

$$E_G = c_1 g^2 + c_2 g^4 + c_3 g^6 + \dots \quad (9)$$

The n -loop coefficient can be written as $c_n = c_n^G + c_n^F$ where c_n^G is the contribution of diagrams without fermion loops and c_n^F comes from diagrams containing fermions. The coefficients c_n^G have been known for some time up to 3 loops [11] (also in 3 dimensions [12], where they are applied to “Magnetostatic” QCD [13] and to dimensionally reduced QCD [14,15]). Independent estimates of higher loop coefficients have also been obtained using stochastic

perturbation theory [16]. The fermionic coefficients c_n^F are known to 2 loops for overlap fermions [17] and up to 3 loops for Wilson fermions [4]; in the present work we extend this computation to the clover action.

The calculation of c_n proceeds most conveniently by computing first the free energy $-(\ln Z)/V$, where Z is the full partition function:

$$Z \equiv \int [\mathcal{D}U \mathcal{D}\bar{\psi}_i \mathcal{D}\psi_i] \exp(-S) \quad (10)$$

Then, E_G is extracted through

$$E_G = -\frac{1}{6} \frac{\partial}{\partial \beta} \left(\frac{\ln Z}{V} \right) \quad (11)$$

In particular, the perturbative expansion of $(\ln Z)/V$:

$$(\ln Z)/V = d_0 - \frac{3(N_c^2-1)}{2} \ln \beta + \frac{d_1}{\beta} + \frac{d_2}{\beta^2} + \dots \quad (12)$$

leads immediately to the relations:

$$c_2 = d_1/(24N_c^2), \quad c_3 = d_2/(24N_c^3) \quad (13)$$

II. CALCULATION AND RESULTS

A Total of 62 Feynman diagrams contribute to the present calculation, up to three loops. The first 36 diagrams are totally gluonic, and the others have both gluon and fermion contributions; these are shown in Appendix A. The involved algebra of lattice perturbation theory was carried out using our computer package in Mathematica. The value for each diagram is computed numerically for a sequence of finite lattices, with typical size $L \leq 36$.

Certain diagrams must be grouped into infrared-finite sets, before extrapolating their values to infinite lattice size (diagrams 11+12+13, 22 through 36, 43+53, 44+52+58, 46+56, 51+57, 55+60, 61+62). Extrapolation leads to a (small) systematic error, which is estimated quite accurately; a consise description of the procedure is provided in Ref. [12].

Diagrams in the shape of a triangular pyramid (18, 19, 20, 49, 50) are the most CPU demanding, since integration over the 3 loop momenta cannot be factorized; these diagrams were necessarily evaluated for smaller L , but fortunately $L \sim 16$ was already sufficient for a very stable extrapolation in these cases. Diagram 40 vanishes identically by color antisymmetry.

The pure gluon contributions are already known [11]:

$$\begin{aligned} c_1^G &= \frac{N_c^2-1}{8 N_c}, \\ c_2^G &= (N_c^2-1) \left(0.0051069297 - \frac{1}{128 N_c^2} \right), \\ c_3^G &= (N_c^2-1) \left(\frac{0.0023152583(50)}{N_c^3} - \frac{0.002265487(17)}{N_c} + 0.000794223(19) N_c \right) \end{aligned} \quad (14)$$

Fermion contributions take the form:

$$\begin{aligned}
c_1^F &= 0, \\
c_2^F &= (N_c^2 - 1) h_2 \frac{N_f}{N_c}, \\
c_3^F &= (N_c^2 - 1) \left(h_{30} N_f + h_{31} \frac{N_f}{N_c^2} + h_{32} \frac{N_f^2}{N_c} \right)
\end{aligned} \tag{15}$$

The coefficients $h_2, h_{30}, h_{31}, h_{32}$ depend polynomially on the clover parameter c_{SW} :

$$h_2 = h_2^{(0)} + h_2^{(1)} c_{\text{SW}} + h_2^{(2)} c_{\text{SW}}^2 \tag{16}$$

$$h_{3i} = h_{3i}^{(0)} + h_{3i}^{(1)} c_{\text{SW}} + h_{3i}^{(2)} c_{\text{SW}}^2 + h_{3i}^{(3)} c_{\text{SW}}^3 + h_{3i}^{(4)} c_{\text{SW}}^4$$

We have calculated $h_2^{(j)}, h_{3i}^{(j)}$ for typical values of the Lagrangian (unrenormalized) fermion mass parameter m , which is connected to the familiar hopping expansion parameter $\kappa = 1/(2m + 8)$. Our results are listed in Appendix B. A complete *per diagram* breakdown of the results would be far too lengthy to present; instead, for potential comparisons, we provide in Appendix B a breakdown only for a particular value of m .

In Figs. 1 and 2 we present the dependence of c_2 and c_3 , respectively, on m , for three typical values of c_{SW} .

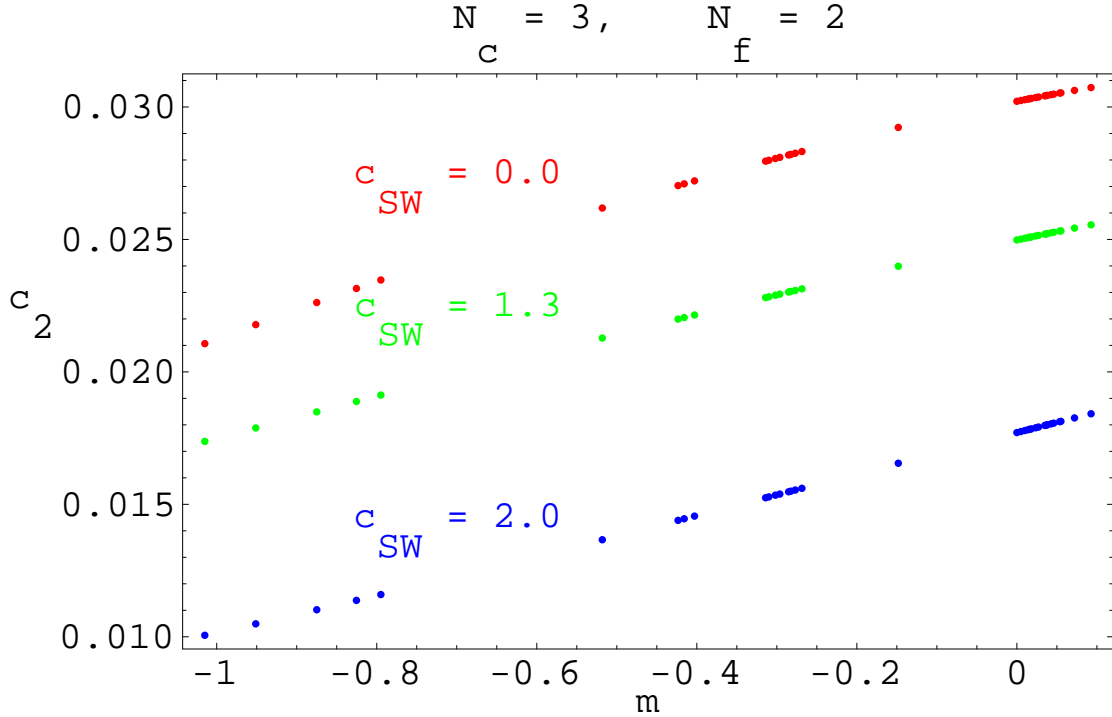


Fig. 1. The dependence of c_2 on the fermion mass m , for some standard values of c_{SW} . $N_c = 3$, $N_f = 2$.

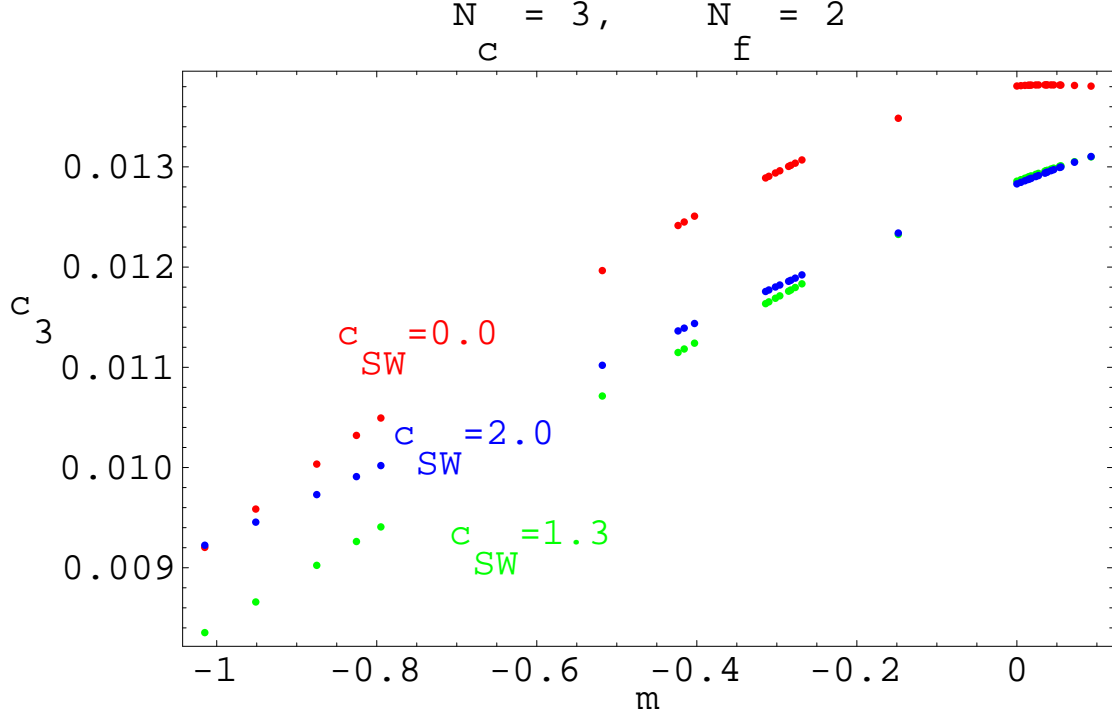


Fig. 2. The dependence of c_3 on the fermion mass m , for some standard values of c_{SW} . $N_c = 3$, $N_f = 2$.

We list below some examples of values for E_G , setting $N_c = 3$. For $N_f = 0$ we have:

$$E_G = (1/3) g^2 + 0.0339109931(3) g^4 + 0.0137063(2) g^6 \quad (17)$$

For two degenerate flavors ($N_f = 2$) and $m = -0.518106$ (corresponding to $\kappa = (8+2m)^{-1} = 0.1436$):

$$\begin{aligned} c_{\text{SW}} = 0.0 : E_G &= (1/3) g^2 + 0.026185200(3) g^4 + 0.0119649(3) g^6, \\ c_{\text{SW}} = 2.0 : E_G &= (1/3) g^2 + 0.013663456(3) g^4 + 0.0110200(13) g^6 \end{aligned} \quad (18)$$

For $N_f = 2$ and $m = 0.038$:

$$\begin{aligned} c_{\text{SW}} = 0.0 : E_G &= (1/3) g^2 + 0.030438866(3) g^4 + 0.0138181(2) g^6, \\ c_{\text{SW}} = 1.3 : E_G &= (1/3) g^2 + 0.025219798(9) g^4 + 0.0129659(5) g^6, \\ c_{\text{SW}} = 2.0 : E_G &= (1/3) g^2 + 0.01800170(1) g^4 + 0.012948(1) g^6 \end{aligned} \quad (19)$$

It is seen that the 3-loop coefficients are quite pronounced for typical values of g used in numerical simulations. For convenience, the behaviour of E_G versus β is also presented in Fig. 3, for the same parameter values as in Eqs. (18,19).

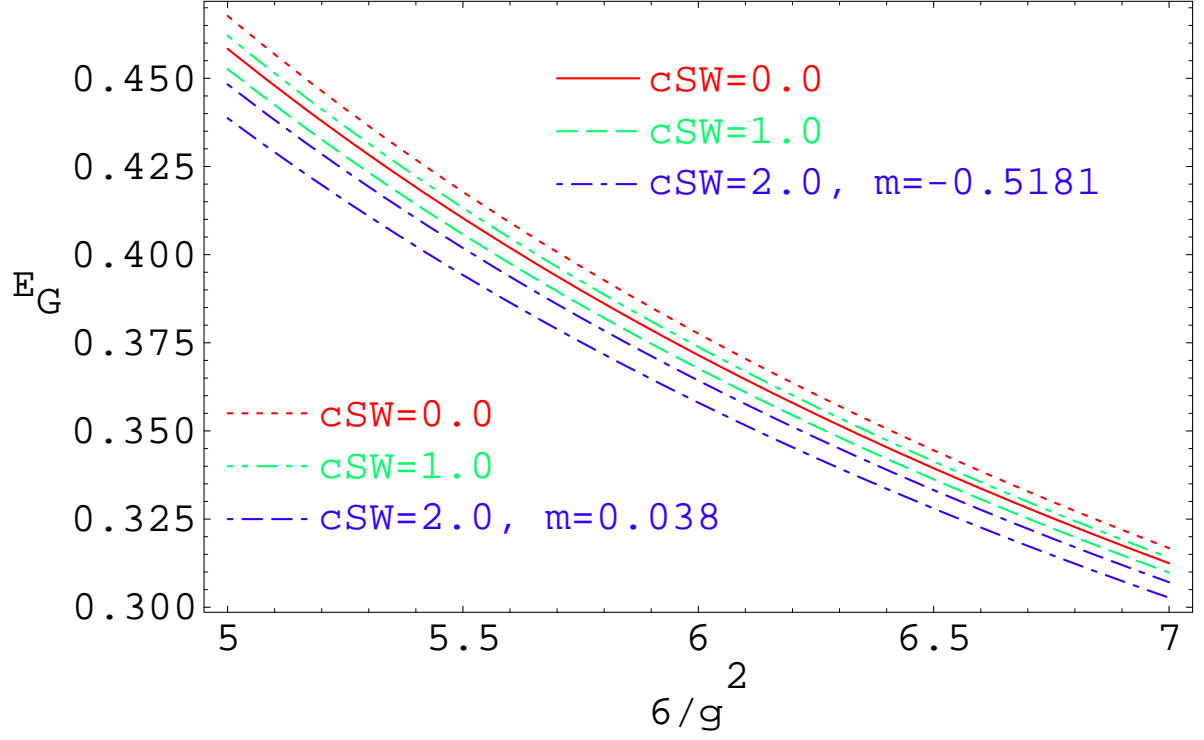


Fig. 3. E_G as a function of β , for $N_c = 3$, $N_f = 2$, and specific mass values.

The detailed results, tabulated in Appendix B for arbitrary values of N_c , N_f , c_{SW} , show a very smooth behaviour as a function of m ; consequently, one is able to reconstruct E_G also for arbitrary values of m by naive interpolation, to excellent precision.

REFERENCES

- [1] B. Sheikholeslami and R. Wohlert, Nucl. Phys. **B259**, 572 (1985).
- [2] CP-PACS/JLQCD Collaborations: T. Ishikawa et al., arXiv:0704.1937.
- [3] UKQCD/SCS Collaboration: M. Göckeler et al., arXiv:0709.3370.
- [4] B. Allés, A. Feo, H. Panagopoulos, Phys. Lett. B **426**, 361 (1998).
- [5] G. Parisi, in: High-Energy Physics – 1980, XX Int. Conf., Madison (1980), ed. L. Durand and L. G. Pondrom (American Institute of Physics, New York, 1981).
- [6] G. P. Lepage and P. B. Mackenzie, Phys. Rev. **D48**, 2250 (1993) [hep-lat/9209022].
- [7] A. Di Giacomo, G. C. Rossi, Phys. Lett. **B100**, 481 (1981).
- [8] G. Bali, P. Boyle, arXiv:hep-lat/0210033.
- [9] M. Lüscher, S. Sint, R. Sommer, P. Weisz and U. Wolff, Nucl. Phys. **B491**, 323 (1997) [hep-lat/9609035].
- [10] H. Kawai, R. Nakayama and K. Seo, Nucl. Phys. **B189**, 40 (1981).
- [11] B. Allés, M. Campostrini, A. Feo, H. Panagopoulos, Phys. Lett. B **324**, 433 (1994).
- [12] H. Panagopoulos, A. Skouroupathis and A. Tsapalis, Phys. Rev. **D73**, 054511 (2006) [hep-lat/0601009].
- [13] A. Hietanen, K. Kajantie, M. Laine, K. Rummukainen and Y. Schröder, PoS (LAT2005) 174 [hep-lat/0509107].
- [14] E. Braaten, Phys. Rev. Lett. **74**, 2164 (1995); E. Braaten and A. Nieto, Phys. Rev. **D53**, 3421 (1996) [hep-ph/9510408].
- [15] A. D. Linde, Rep. Prog. Phys. **42**, 389 (1979); Phys. Lett. **B96**, 289 (1980).
- [16] C. Torrero, F. Di Renzo, V. Miccio, M. Laine, Y. Schröder, PoS (LAT2005) 189 [hep-lat/0509157], and references therein.
- [17] A. Athenodorou and H. Panagopoulos, Phys. Rev. **D70**, 077507 (2004) [hep-lat/0408020].

APPENDIX A

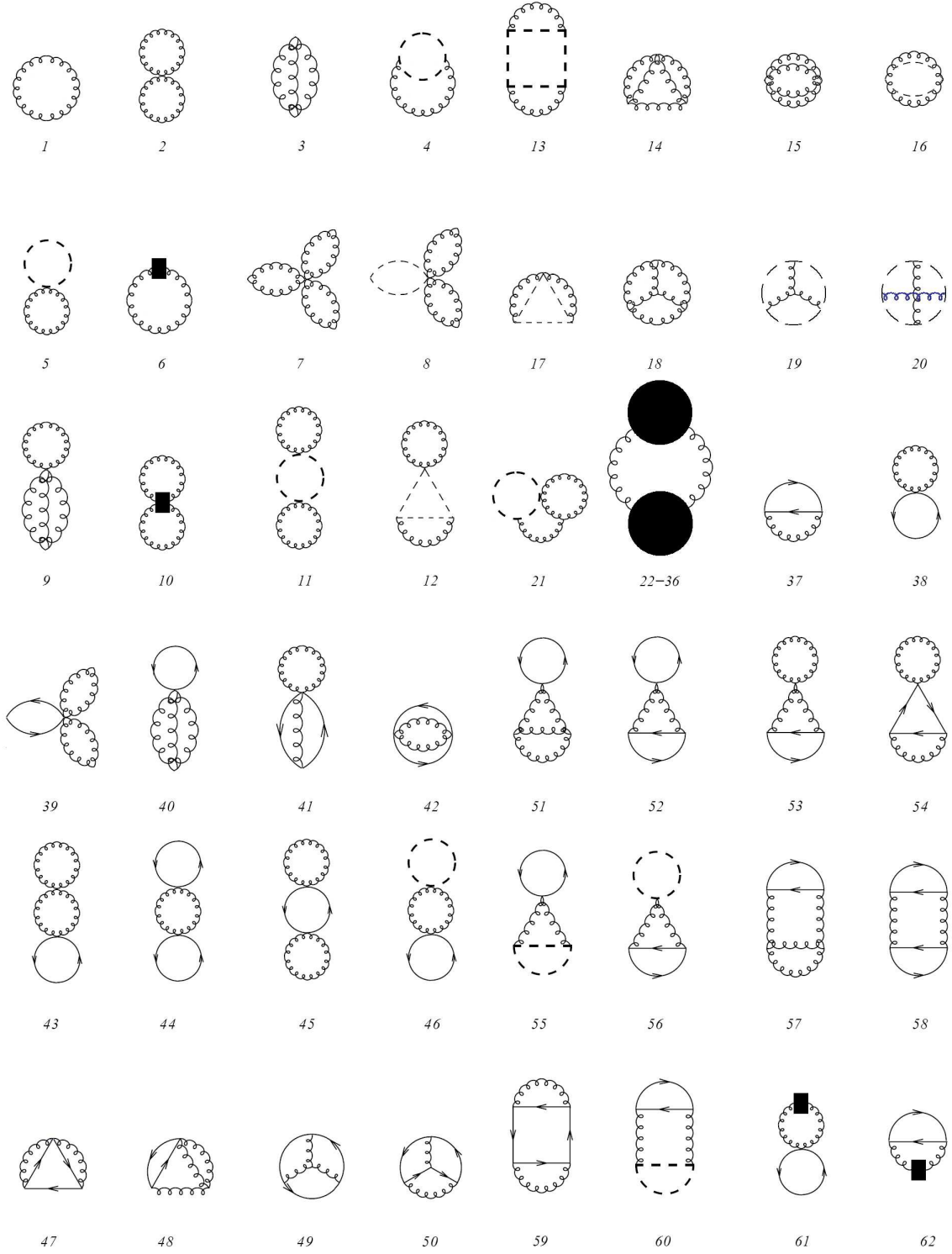


Fig. 4. Feynman diagrams contributing to the free energy, at one, two, and three loops.

Figure 4 depicts all diagrams contributing to the free energy at 1 loop (diagram 1), 2 loops (2-6, 37-38), and 3 loops (7-36, 39-62). Solid (curly, dashed) lines represent fermions (gluons, ghosts), and the filled square is the contribution from the measure part of the action. The filled circle, corresponding to the non-fermionic part of the 1-loop gluon self-energy, is given in Figure 5.

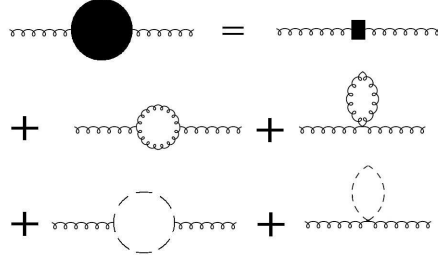


Fig. 5. Non-fermionic diagrams renormalizing the gluon propagator at 1 loop.

APPENDIX B

Tables I-IV provide a *per diagram* breakdown of our results, at a given value of m ($m = 0.038$), in order to allow for potential comparisons and cross checks. The total results for the coefficients $h_2^{(j)}$, $h_{30}^{(j)}$, $h_{31}^{(j)}$, $h_{32}^{(j)}$ are listed in Tables V-VIII, respectively, for a wide selection of m values which are used in the literature. Given the smooth dependence of all these coefficients on m , interpolations to other intermediate values of m can be performed with great accuracy.

TABLE I. Per-diagram contributions to $h_2^{(j)}$. $m = 0.038$.

diagram	$h_2^{(0)} \cdot 10^4$	$h_2^{(1)} \cdot 10^4$	$h_2^{(2)} \cdot 10^4$
37	0.932189(6)	0.14684(1)	-5.903340(3)
38	-7.442427121(2)	0	0

TABLE II. Per-diagram contributions to $h_{30}^{(j)}$. $m = 0.038$.

diagram	$h_{30}^{(0)} \cdot 10^4$	$h_{30}^{(1)} \cdot 10^4$	$h_{30}^{(2)} \cdot 10^4$	$h_{30}^{(3)} \cdot 10^4$	$h_{30}^{(4)} \cdot 10^4$
39	0.19218007757(5)	0	0	0	0
41	-0.096284(2)	-0.047087(2)	3.176923(5)	0	0
42	0.00427805(2)	0	-1.303406(1)	0	0
43+53	-1.49693(1)	0.031601(2)	-1.343093(3)	0	0
45	1.574326(1)	0	0	0	0
46+56	0.102791(5)	-0.005620(1)	0.1231742(3)	0	0
47	-0.0006435(4)	-0.0369073(4)	-0.0637549(3)	0.00356648(1)	0
48	0	-0.0000025(1)	-0.0395366(6)	0	0
49	0.12905(6)	-0.01919(3)	-0.017117(8)	-0.0078566(7)	0
51+57	-0.37601(2)	0.023672(5)	-0.4837191(5)	0	0
54	-0.24831(4)	-0.3910(2)	-0.41414(8)	0	0
55+60	0.028358(1)	-0.0017428(5)	0.03556619(6)	0	0
59	0.012859(2)	0.01395(1)	0.07042(2)	0.05069(3)	-0.020929(8)
61+62	0.20558(1)	-0.011239(2)	0.2463485(6)	0	0

 TABLE III. Per-diagram contributions to $h_{31}^{(j)}$. $m = 0.038$.

diagram	$h_{31}^{(0)} \cdot 10^4$	$h_{31}^{(1)} \cdot 10^4$	$h_{31}^{(2)} \cdot 10^4$	$h_{31}^{(3)} \cdot 10^4$	$h_{31}^{(4)} \cdot 10^4$
39	-0.2882701164(1)	0	0	0	0
41	0.144427(2)	0.048077(2)	-2.951676(8)	0	0
42	-0.00855609(4)	0	0	0	0
43+53	1.62756(1)	-0.036704(2)	1.475838(3)	0	0
45	-1.574326(1)	0	0	0	0
47	0.0012870(5)	0.0073718(6)	0.0042472(4)	0	0
50	-0.0096(1)	-0.02767(1)	0.01081(4)	0.000361(3)	-0.007025(2)
54	0.24831(5)	0.3910(2)	0.41414(8)	0	0
59	-0.012859(2)	-0.01395(2)	-0.07042(2)	-0.05069(3)	0.020929(8)

 TABLE IV. Per-diagram contributions to $h_{32}^{(j)}$. $m = 0.038$.

diagram	$h_{32}^{(0)} \cdot 10^6$	$h_{32}^{(1)} \cdot 10^6$	$h_{32}^{(2)} \cdot 10^6$	$h_{32}^{(3)} \cdot 10^6$	$h_{32}^{(4)} \cdot 10^6$
44+52+58	3.65818(5)	-0.24532(8)	7.62942(7)	-0.41017(3)	5.742740(1)

TABLE V. Total values of $h_2^{(j)}$, for various masses.

m	$h_2^{(0)} \cdot 10^3$	$h_2^{(1)} \cdot 10^3$	$h_2^{(2)} \cdot 10^3$
-1.014925	-2.4083635(4)	0.395934967(3)	-0.71409763(8)
-0.9512196	-2.2738528(3)	0.359466059(5)	-0.70919125(2)
-0.8749999	-2.1173032(2)	0.318089891(2)	-0.70272042(1)
-0.8253968	-2.0179859(2)	0.292493808(2)	-0.698193815(6)
-0.7948719	-1.9578750(2)	0.277266040(2)	-0.695294722(3)
-0.5181059	-1.4485862(6)	0.15739842(6)	-0.66565598(2)
-0.423462	-1.2897989(2)	0.1238792(6)	-0.6543190(2)
-0.4028777	-1.2563603(3)	0.1170884(9)	-0.6517790(3)
-0.3140433	-1.1167334(5)	0.089818(2)	-0.6405147(6)
-0.301775	-1.0980649(6)	0.086312(1)	-0.6389201(5)
-0.2962964	-1.0897779(5)	0.084766(2)	-0.6382049(7)
-0.2852897	-1.0732218(2)	0.081700(5)	-0.636761(3)
-0.2769916	-1.0608234(1)	0.079422(6)	-0.635665(4)
-0.2686568	-1.0484419(4)	0.077161(3)	-0.634562(4)
-0.1482168	-0.8779913(3)	0.04774(1)	-0.618118(2)
0.	-0.6929202(1)	0.02010061(2)	-0.59630769(1)
0.038	-0.6510238(6)	0.014684(1)	-0.5903340(3)
0.072	-0.615948(1)	0.010488(4)	-0.584812(2)
0.0927	-0.5956994(5)	0.008214(2)	-0.5813703(7)

 TABLE VI. Total values of $h_{30}^{(j)}$, for various masses.

m	$h_{30}^{(0)} \cdot 10^4$	$h_{30}^{(1)} \cdot 10^4$	$h_{30}^{(2)} \cdot 10^4$	$h_{30}^{(3)} \cdot 10^4$	$h_{30}^{(4)} \cdot 10^4$
-1.014925	-3.61593(9)	-0.5205(4)	-0.16938(2)	0.18044(3)	-0.01301953(3)
-0.9512196	-3.30186(3)	-0.5660(4)	-0.16042(2)	0.17452(3)	-0.01362776(1)
-0.8749999	-2.93686(3)	-0.6119(4)	-0.15115(2)	0.16699(4)	-0.014206930(3)
-0.8253968	-2.70587(4)	-0.6368(5)	-0.14582(2)	0.16186(4)	-0.014512957(7)
-0.7948719	-2.56636(4)	-0.6503(5)	-0.14275(1)	0.15863(4)	-0.01467848(1)
-0.5181059	-1.4032(2)	-0.7097(3)	-0.1185(1)	0.126761(7)	-0.01575561(2)
-0.423462	-1.0538(3)	-0.7039(1)	-0.1097(1)	0.11495(2)	-0.016111(1)
-0.4028777	-0.9817(2)	-0.7010(1)	-0.10756(6)	0.11233(2)	-0.016198(2)
-0.3140433	-0.6879(1)	-0.6810(1)	-0.0971(1)	0.100645(8)	-0.016638(4)
-0.301775	-0.6497(1)	-0.6770(3)	-0.0956(1)	0.09905(3)	-0.016708(4)
-0.2962964	-0.6329(1)	-0.6751(2)	-0.0948(1)	0.09828(5)	-0.016735(8)
-0.2852897	-0.5994(1)	-0.6719(4)	-0.0934(1)	0.09675(5)	-0.01681(1)
-0.2769916	-0.5746(1)	-0.6686(5)	-0.0921(2)	0.09565(5)	-0.016868(9)
-0.2686568	-0.54989(8)	-0.6653(5)	-0.0907(2)	0.09458(3)	-0.016911(8)
-0.1482168	-0.23130(6)	-0.6101(4)	-0.0704(2)	0.07775(9)	-0.01785(2)
0.	0.01867(6)	-0.49191(1)	-0.02955(1)	0.053914(1)	-0.01998581(2)
0.038	0.03126(8)	-0.4436(2)	-0.01234(8)	0.04640(3)	-0.020929(8)
0.072	0.03095(9)	-0.3997(2)	0.00431(7)	0.03982(2)	-0.021807(5)
0.0927	0.02828(7)	-0.3744(3)	0.0144(1)	0.03610(3)	-0.022300(6)

TABLE VII. Total values of $h_{31}^{(j)}$, for various masses.

m	$h_{31}^{(0)} \cdot 10^4$	$h_{31}^{(1)} \cdot 10^4$	$h_{31}^{(2)} \cdot 10^4$	$h_{31}^{(3)} \cdot 10^4$	$h_{31}^{(4)} \cdot 10^4$
-1.014925	4.2718(2)	0.61383(4)	-1.1331(2)	-0.18127(4)	0.002886(2)
-0.9512196	3.9078(2)	0.636745(4)	-1.1391(2)	-0.17467(4)	0.003690(2)
-0.8749999	3.4867(2)	0.65829(6)	-1.1434(2)	-0.16655(3)	0.004505(1)
-0.8253968	3.2212(2)	0.6689(1)	-1.1447(2)	-0.16119(3)	0.004966(1)
-0.7948719	3.0614(2)	0.6741(1)	-1.1450(2)	-0.15783(3)	0.005226(1)
-0.5181059	1.7413(2)	0.6750(2)	-1.1343(1)	-0.12639(1)	0.007141(2)
-0.423462	1.3494(2)	0.6559(1)	-1.12732(6)	-0.11512(2)	0.007770(1)
-0.4028777	1.2686(2)	0.6503(1)	-1.12575(6)	-0.11264(1)	0.007917(2)
-0.3140433	0.9409(2)	0.6207(1)	-1.11893(5)	-0.10162(2)	0.008611(6)
-0.301775	0.8984(2)	0.6156(3)	-1.1180(1)	-0.10013(4)	0.008715(5)
-0.2962964	0.8797(2)	0.6132(1)	-1.1176(1)	-0.09941(6)	0.008759(8)
-0.2852897	0.8424(2)	0.6090(3)	-1.1168(1)	-0.09798(5)	0.00887(1)
-0.2769916	0.8147(2)	0.6050(4)	-1.1163(2)	-0.09695(6)	0.00895(1)
-0.2686568	0.7872(2)	0.6011(4)	-1.1159(2)	-0.09594(3)	0.009012(8)
-0.1482168	0.4324(2)	0.5382(4)	-1.1090(2)	-0.0801(1)	0.01029(2)
0.	0.1479(2)	0.41633(5)	-1.11100(1)	-0.057537(3)	0.01284418(4)
0.038	0.1279(1)	0.3681(2)	-1.1171(1)	-0.05033(3)	0.013904(9)
0.072	0.1221(1)	0.3248(2)	-1.1232(1)	-0.04400(2)	0.014891(5)
0.0927	0.1211(1)	0.3000(3)	-1.1268(1)	-0.04044(3)	0.015451(6)

 TABLE VIII. Total values of $h_{32}^{(j)}$, for various masses.

m	$h_{32}^{(0)} \cdot 10^4$	$h_{32}^{(1)} \cdot 10^4$	$h_{32}^{(2)} \cdot 10^4$	$h_{32}^{(3)} \cdot 10^4$	$h_{32}^{(4)} \cdot 10^4$
-1.014925	0.49011557(4)	-0.19966299(3)	0.36828835(3)	-0.11015360(1)	0.08360193(2)
-0.9512196	0.43836868(2)	-0.17353447(1)	0.343436025(6)	-0.10025167(1)	0.082274351(7)
-0.8749999	0.38167686(2)	-0.14550571(1)	0.31500822(1)	-0.088919069(7)	0.080600027(9)
-0.8253968	0.34767753(1)	-0.129038814(4)	0.297262047(4)	-0.081862310(7)	0.079469961(8)
-0.7948719	0.327840761(5)	-0.119564143(4)	0.286632961(4)	-0.077648919(7)	0.078761444(7)
-0.5181059	0.18222240(4)	-0.0539075(2)	0.20003143(6)	-0.04416150(5)	0.072038437(4)
-0.423462	0.1450777(2)	-0.0386899(4)	0.1742885(2)	-0.0347205(4)	0.06966149(6)
-0.4028777	0.1377609(1)	-0.0357991(4)	0.1689417(2)	-0.0328053(6)	0.0691407(1)
-0.3140433	0.1091234(3)	-0.0249053(4)	0.1468864(3)	-0.025111(1)	0.0668770(3)
-0.301775	0.1055301(5)	-0.023593(2)	0.1439703(7)	-0.024122(3)	0.0665614(9)
-0.2962964	0.1039530(7)	-0.023021(2)	0.1426783(9)	-0.023686(3)	0.0664209(8)
-0.2852897	0.1008352(9)	-0.021900(2)	0.1401015(9)	-0.022821(1)	0.0661380(3)
-0.2769916	0.0985290(7)	-0.021075(1)	0.1381755(8)	-0.022178(4)	0.0659243(2)
-0.2686568	0.0962507(4)	-0.020271(6)	0.1362553(5)	-0.021542(4)	0.0657091(3)
-0.1482168	0.0674197(9)	-0.010680(4)	0.1101470(8)	-0.013260(4)	0.062561(1)
0.	0.04159747(5)	-0.00356316(1)	0.08245984(4)	-0.005574256(7)	0.058518838(6)
0.038	0.0365818(5)	-0.0024532(8)	0.0762942(7)	-0.0041017(3)	0.05742740(1)
0.072	0.0326353(4)	-0.001675(1)	0.071174(1)	-0.0029808(5)	0.0564209(3)
0.0927	0.0304618(8)	-0.0012878(2)	0.0682377(9)	-0.002377(2)	0.0557953(1)